Available online at www.sciencedirect.com
SCIENCE DIRECT
Polymer 47 (2006) 6187–6201
polymer
www.elsevier.com/locate/polymer

Blown films of nanocomposites prepared from low density polyethylene and a sodium ionomer of poly(ethylene-*co*-methacrylic acid)

Rhutesh K. Shah [a,*], Rajendra K. Krishnaswamy [b], Shuichi Takahashi [a], D.R. Paul [a,*]

[a] *Department of Chemical Engineering and Texas Materials Institute, The University of Texas at Austin, Austin, TX 78712-1062, USA*
[b] *Chevron Phillips Chemical Company, Bartlesville Technology Center, Bartlesville, OK 74004, USA*

Received 26 May 2006; accepted 22 June 2006
Available online 10 July 2006

Abstract

A detailed study of the performance of blown films prepared from nanocomposites based on LDPE and a sodium ionomer of poly(ethylene-*co*-methacrylic acid) is reported. The organoclay content and film blowing conditions were varied to determine the effect of platelet concentration, exfoliation and orientation on film properties. Mechanical properties including stiffness, puncture resistance, and resistance to tear propagation were evaluated and compared to corresponding properties of unfilled polymer films. Permeability of the films to moisture and common atmospheric gases like oxygen, nitrogen, and carbon dioxide was also measured using standard testing methods.

In general, films prepared from nanocomposites based on the ionomer exhibited greater improvements in mechanical and barrier properties over unfilled polymer compared to similar films prepared from nanocomposites based on LDPE. This is due to the greater degree of organoclay exfoliation achieved in the ionomer compared to LDPE. The addition of 3 wt% MMT to the ionomer increased the tensile modulus of blown films by an average of 50% without sacrificing much tear strength, puncture resistance or film extensibility. Gas permeability in these films was lowered by 40% and moisture transmission rate was reduced by 60%.

Keywords: Blown films; Nanocomposite; Polyethylene

1. Introduction

Polymer-layered silicate nanocomposites prepared from the organically modified clay mineral montmorillonite (MMT) are of increasing interest for packaging applications [1–8]. These composites offer the promise of improved mechanical and barrier properties over those of the matrix polymer owing to the nanoscale reinforcement and the tortuous diffusion path caused by dispersing the 1 nm thick, high aspect ratio aluminosilicate (clay) layers. In order to maximize these benefits it is necessary to attain high levels of organoclay exfoliation accompanied by a uniform distribution and proper orientation of the clay platelets. The formation of such nanocomposites from widely used, low-cost packaging polymers like low density polyethylene (LDPE) is of specific interest. Unfortunately, LDPE is highly inefficient at exfoliating the organoclays, since there is no favorable interaction with the polar surface of the clay [9–11]. While complete exfoliation of the organoclay in LDPE seems impossible, it is possible to improve the level of filler dispersion by carefully engineering the structure of the surfactant (surface treatment) used for preparing the organoclay [10,11].

In contrast, ionomers, prepared by copolymerizing LDPE with small amounts of methacrylic acid (~5 mol%) followed by neutralization of some of the acid groups by metal bases [12], do a much better job of exfoliating these organoclays [10,13,14]. This has been attributed to the interactions of the ionic and acid groups in these polymers with the aluminosilicate surface of the clay. Such ionomers are widely used in a variety of packaging applications because of their clarity, barrier properties, high hot tack strength, low sealing temperatures, high clarity, and good formability [15].

* Corresponding authors. Tel.: +1 512 471 5392; fax: +1 512 471 0542.
E-mail addresses: rhutesh@che.utexas.edu (R.K. Shah), drp@che.utexas.edu (D.R. Paul).

0032-3861/$ - see front matter © 2006 Elsevier Ltd. All rights reserved.
doi:10.1016/j.polymer.2006.06.051

In this study, we have evaluated the physical and barrier properties of blown films of nanocomposites prepared by melt mixing a suitable organoclay with LDPE and a sodium ionomer of poly(ethylene-*co*-methacrylic acid). The selection of these two polymers, thus, allows us a comparison of two systems that exhibit quite different levels of exfoliation. The choice of the film preparation method (film blowing as opposed to casting, compression molding, etc.) was dictated by the possibility of greater biaxial orientation of the platelets/agglomerates in films made by this process. The organoclay structure and melt processing conditions were optimized to form nanocomposites with acceptable levels of exfoliation. Films with thicknesses of 1 mil, 2 mil, and 3 mil were prepared by varying the draw down ratio at two different blow-up ratios to determine the effect of platelet concentration, exfoliation, and orientation on film performance. Mechanical properties including stiffness, puncture resistance, and resistance to tear propagation were evaluated and compared to corresponding properties of unfilled polymer films. Permeability of the films to moisture and common atmospheric gases like oxygen, nitrogen and carbon dioxide was also measured using standard testing methods.

2. Experimental

A commercially available grade of LDPE, Novapol LF-0219A, and a sodium ionomer of poly(ethylene-*co*-methacrylic acid), Surlyn® 8945 were used in this study. Selected properties of these materials are included in Table 1. The melting point and heat of fusion of the polymers were determined using DSC analysis, while, their crystallinity was calculated by dividing the respective heats of fusion by the heat of fusion for 100% crystalline polyethylene, 293 J/g [16]. DSC analyses were made with a Perkin Elmer DSC 7 using 10 mg of polymer excised from pellets. All samples were initially heated to 180 °C at 40 °C/min, held at that temperature for 5 min, and subsequently cooled to 0 °C at 5 °C/min. After holding at 0 °C for 3 min, the samples were reheated to 180 °C at 20 °C/min. The values reported in Table 1 were recorded on the second heating. The organically modified clay, designated here as $M_2(HT)_2$-140, was supplied by Southern Clay Products and was used as received. It was prepared by a cation exchange reaction between sodium montmorillonite and a two-tailed quaternary ammonium surfactant, dimethyl bis(hydrogenated-tallow) ammonium chloride (Arquad 2HT-75). The suffix 140 represents the MER loading level of the organoclay (see Table 1 for details), i.e., the clay is over-exchanged and the excess amine is within the galleries of the as-received organoclay. The choice of the organoclay was based upon recent studies exploring the effect of the surfactant structure on organoclay exfoliation in polyethylene [9–11] and the selected sodium ionomer of poly(ethylene-*co*-methacrylic acid) [13]. These studies revealed that higher levels of organoclay exfoliation could be achieved using surfactants with multiple alkyl tails on the ammonium ion rather than one tail and by using organoclays with excess surfactant rather than stoichiometric loading. This is believed to be the result of the better affinity these polymers have for the largely aliphatic organic modifier than for the pristine surface of the clay. In addition, the larger the number of alkyl tails, or larger the amount of surfactant, the more the silicate surface is shielded from the matrix; this combination of factors leads to better exfoliation of the organoclay.

Table 1
Materials used in this study

Material	Commercial designation	Specifications	Supplier
Low density polyethylene (LDPE)	Novapol® LF-0219A	MI = 2.3 g/10 min Specific gravity = 0.919 Melting point[a] = 109.7 °C Heat of fusion[a] = 128.4 J/g Crystallinity[a] = 42.7%	Nova Chemicals Corporation
Sodium ionomer of poly(ethylene-*co*-methacrylic acid)	Surlyn® 8945	MI = 4.5 g/10 min Specific gravity = 0.96 Methacrylic acid content = 15.2 wt% Sodium content = 1.99 wt% Neutralization = ~40% Melting point[a] = 90.1 °C Heat of fusion[a] = 54.8 J/g Crystallinity[a] = 18.7%	E.I. du Pont de Nemours and Company
Organoclay[b]: dimethyl bis(hydrogenated-tallow) ammonium montmorillonite	Cloisite® 6A	Organic loading[c] = 140 MER Organic content = 48.0 wt% d_{001} spacing[d] = 35.1 Å	Southern clay products

[a] The melting point and heat of fusion were determined using DSC analysis. The crystallinity of the polymer was calculated by dividing the heat of fusion of the polymer by 293 J/g, the heat of fusion estimated for 100% crystalline polyethylene [16].

[b] The selected organoclay is designated as $M_2(HT)_2$-140 in this study, where M = methyl and HT = hydrogenated tallow. Tallow is a natural product composed predominantly (63%) of saturated and unsaturated C_{18} chains. HT is the saturated form yet still contains a small fraction of double bonds.

[c] The organic loading describes the number of milliequivalents of amine salt used per 100 g of clay (MER) during the cation exchange reaction with sodium montmorillonite.

[d] The basal spacing corresponds to the characteristic Bragg reflection peak d_{001} obtained from a powder WAXS scan of the organoclay.

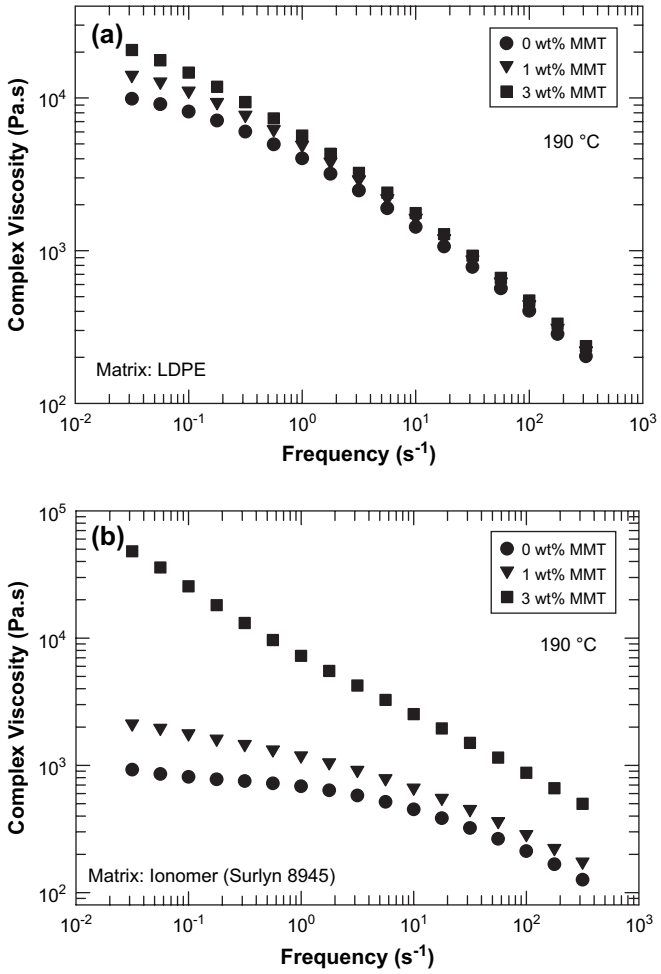

Fig. 1. Complex viscosity of the unfilled polymers and nanocomposites prepared from (a) LDPE and (b) a sodium ionomer of poly(ethylene-*co*-methacrylic acid), Surlyn® 8945.

The polymers and the organoclay were melt mixed in a Werner–Pfleiderer ZSK25 twin screw co-rotating extruder ($D = 25$ mm, $L/D = 48$) at 190 °C, using a feed rate of 40 lb/h to form nanocomposites with 1 and 3 wt% MMT. The filler and the matrix were added to the extruder using two separate feed-ports. Polymer was fed using an upstream port while the clay was added to the molten polymer using a downstream port. Prior experience [17,18] has revealed better organoclay exfoliation in nanocomposites formed using such a feeding system, rather than feeding the clay and the polymer together in the upstream region of the extruder, which mainly consists of kneading blocks.

Blown films were prepared from the polymers and their nanocomposites at 190 °C using a 38 mm Davis Standard extruder fitted with a 10.16 cm Sano Spiral-Mandrel film die and a dual lip-air ring, at two different blow-up ratios (BUR), 2:1 and 3:1. The draw down ratio (DDR) was varied to form films with 1 mil, 2 mil, and 3 mil thicknesses, respectively (1 mil = 25.4 μm). BUR, a term commonly used in describing the processing conditions for blown films, is the ratio of the diameter of the final film 'tube' to the diameter of the die. DDR, another such term, is the ratio of the final film velocity, i.e., the velocity at the nip roll, to the initial polymer velocity, i.e., the average polymer velocity at the die exit. DDR and BUR are correlated by a simple mathematical equation: DDR = (Die gap)/[(film thickness) × (BUR)]. In all, 35 films were blown; it was not possible to blow film from the unfilled ionomer at one condition (3:1 BUR and 7 DDR) as bubble stability could not be maintained. Puncture resistance (dart impact strength), tensile properties, and resistance to tear propagation of the nanocomposite films in the machine direction (MD) and transverse direction (TD) were evaluated as per ASTM standards D1709, D882, and D1922, respectively, and the properties were compared to those of the corresponding unfilled polymer films. Permeability of the films to O_2, N_2 and CO_2 gases were determined at 35 °C using a constant-volume-variable pressure method as described by Koros et al. [19]. The thickness of each film sample used for permeability measurements was confirmed using a micrometer screw. Moisture permeability of the films was determined as per ASTM standard F1249.

Melt rheological measurements of the nanocomposites were made using an ARES torsional rheometer operated in an oscillatory mode at 190 °C in a nitrogen atmosphere. Compression molded disks (~1.8–2.0 mm) were placed between the parallel plates of the rheometer. Once thermal equilibrium was achieved, the disks were squeezed between the parallel plates to 1.6 mm thickness, and the excess material was trimmed prior to the frequency sweep test.

3. Results and discussion

3.1. Rheology of nanocomposites

Complex viscosities of the nanocomposites and the unfilled polymers are presented in Fig. 1. For both polymers, at low frequencies, the melt viscosity increases systematically with increasing clay content. This is consistent with the previous studies examining the rheological behavior of polymer clay

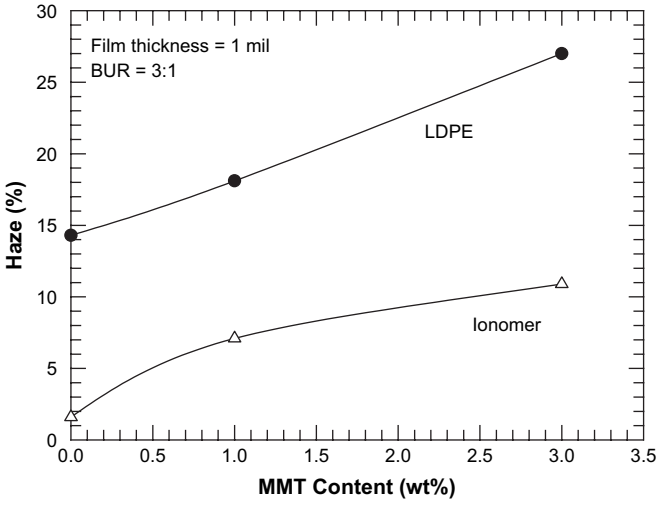

Fig. 2. Percentage haze values of selected blown films prepared from LDPE and the Surlyn® ionomer plotted as a function of the montmorillonite content.

Table 2
Selected mechanical properties of the blown films examined in this study

Film no.	Matrix	MMT (wt%)	BUR	Thickness (mil)	DDR	MD tear (g)	TD tear (g)	Dart impact (g)	Tensile modulus (MPa)		Break stress (MPa)		Break strain (%)	
									MD	TD	MD	TD	MD	TD
1	LDPE	0	2:1	3	10.0	180	148	40	157.8	191.1	16.0	15.0	275.2	564.4
2	LDPE	0	2:1	2	15.0	202	109	42	159.7	191.6	17.9	14.4	221.4	475.2
3	LDPE	0	2:1	1	30.0	362	106	38	184.1	233.6	25.6	12.3	86.3	394.1
4	LDPE	0	3:1	3	6.7	59	126	84	154.5	165.1	15.6	16.4	324.1	502.2
5	LDPE	0	3:1	2	10.0	57	96	87	165.5	172.0	17.4	16.2	251.6	499.0
6	LDPE	0	3:1	1	20.0	104	74	83	188.5	195.2	24.2	15.3	104.4	390.8
7	LDPE	1	2:1	3	10.0	73	152	37	179.5	202.5	17.6	14.6	269.5	541.7
8	LDPE	1	2:1	2	15.0	292	262	45	193.7	229.3	18.7	14.8	171.6	499.2
9	LDPE	1	2:1	1	30.0	290	150	23	212.6	269.2	26.3	11.8	75.5	343.6
10	LDPE	1	3:1	3	6.7	33	113	50	182.2	193.5	15.6	16.1	326.7	529.1
11	LDPE	1	3:1	2	10.0	56	138	72	169.9	200.8	17.0	14.9	228.5	436.1
12	LDPE	1	3:1	1	20.0	43	90	84	202.7	225.8	23.0	14.3	99.6	342.1
13	LDPE	3	2:1	3	10.0	131	181	33	201.8	239.6	17.9	16.4	246.2	600.3
14	LDPE	3	2:1	2	15.0	160	331	35	217.8	268.6	20.0	13.0	139.9	420.5
15	LDPE	3	2:1	1	30.0	11	223	23	236.8	273.2	30.8	11.5	70.7	351.0
16	LDPE	3	3:1	3	6.7	56	144	79	197.6	210.1	15.2	17.4	343.2	512.8
17	LDPE	3	3:1	2	10.0	65	256	59	193.5	199.3	21.7	16.4	222.1	472.9
18	LDPE	3	3:1	1	20.0	84	115	68	219.4	244.5	23.3	14.4	101.4	366.6
19	Ionomer	0	2:1	3	10.0	18	23	274	255.4	261.6	26.9	24.2	252.1	329.5
20	Ionomer	0	2:1	2	15.0	13	23	249	312.5	298.6	29.7	21.0	185.0	253.4
21	Ionomer	0	2:1	1	30.0	9	17	274	252.7	282.3	31.3	19.9	67.4	227.0
22	Ionomer	0	3:1	3	6.7	[a]	[a]	[a]	[a]	[a]	[a]	[a]	[a]	[a]
23	Ionomer	0	3:1	2	10.0	15	16	298	277.0	279.7	24.5	26.5	253.6	275.9
24	Ionomer	0	3:1	1	20.0	17	21	329	296.4	249.4	24.1	26.8	108.0	226.6
25	Ionomer	1	2:1	3	10.0	23	18	250	300.6	302.4	25.8	24.6	238.8	307.2
26	Ionomer	1	2:1	2	15.0	15	19	244	355.2	323.9	27.0	22.5	188.9	251.3
27	Ionomer	1	2:1	1	30.0	9	19	331	335.2	315.5	28.1	20.7	87.5	195.7
28	Ionomer	1	3:1	3	6.7	23	20	164	346.7	348.4	24.3	30.1	275.1	301.7
29	Ionomer	1	3:1	2	10.0	21	17	263	322.2	324.3	25.5	26.6	220.0	241.0
30	Ionomer	1	3:1	1	20.0	15	15	360	326.5	318.8	22.6	24.5	126.6	187.2
31	Ionomer	3	2:1	3	10.0	24	28	196	415.8	385.2	22.8	24.4	251.2	288.9
32	Ionomer	3	2:1	2	15.0	14	21	211	470.3	422.8	26.9	22.3	182.6	232.2
33	Ionomer	3	2:1	1	30.0	11	18	201	440.7	384.2	28.2	19.6	77.3	157.1
34	Ionomer	3	3:1	3	6.7	26	23	178	449.7	434.5	26.7	29.5	266.9	298.2
35	Ionomer	3	3:1	2	10.0	16	17	195	436.1	390.6	24.6	24.6	212.8	236.7
36	Ionomer	3	3:1	1	20.0	14	22	243	432.4	405.4	26.6	22.2	120.4	144.0

[a] It was not possible to blow film #22, as bubble stability could not be maintained.

nanocomposites [20–23]. It is interesting to note that the magnitude of viscosity enhancement for the ionomer based nanocomposites is much greater than for the LDPE based nanocomposites. This is attributable to higher level of organoclay exfoliation in the ionomer based nanocomposites compared to the LDPE based nanocomposites as discussed earlier. In particular, the ionomer nanocomposite with 3 wt% MMT does not reveal a Newtonian plateau (at low shear rates) evident for the pure ionomer and for the nanocomposite containing 1 wt% MMT. This is consistent with the rheological signature for the formation of a network of clay platelets within the ionomer matrix.

3.2. Visual morphology of blown films

The films produced exhibited good surface properties. As expected, samples prepared from the unfilled polymers were colorless, while those prepared from the nanocomposites had a yellowish tinge. All samples had a smooth texture, which was a significant improvement over previous trials when the samples had rough, sand-paper like texture [24]. This could be attributed to the acceptable levels of organoclay exfoliation achieved in these nanocomposites resulting from the use of an appropriate organoclay and optimum processing conditions. The clarity of the films was slightly compromised by the addition of organoclay. As shown in Fig. 2, the haze increases steadily with an increase in the clay content. All of the films produced, including those with the organoclay, contained very few visual imperfections such as gels or fisheyes.

3.3. Mechanical properties of blown films

Selected mechanical properties of the blown films prepared are listed in Table 2.

3.3.1. Tensile modulus

Tensile moduli data of the blown films prepared from LDPE and its nanocomposites are presented in Fig. 3. Similar data for blown films prepared from the Surlyn® ionomer are presented in Fig. 4.

As expected [9,10,13], for both polymers, tensile modulus increases as the organoclay content increases. It is important to note that the modulus enhancement is significant along both the MD and TD of the blown films. The increase in

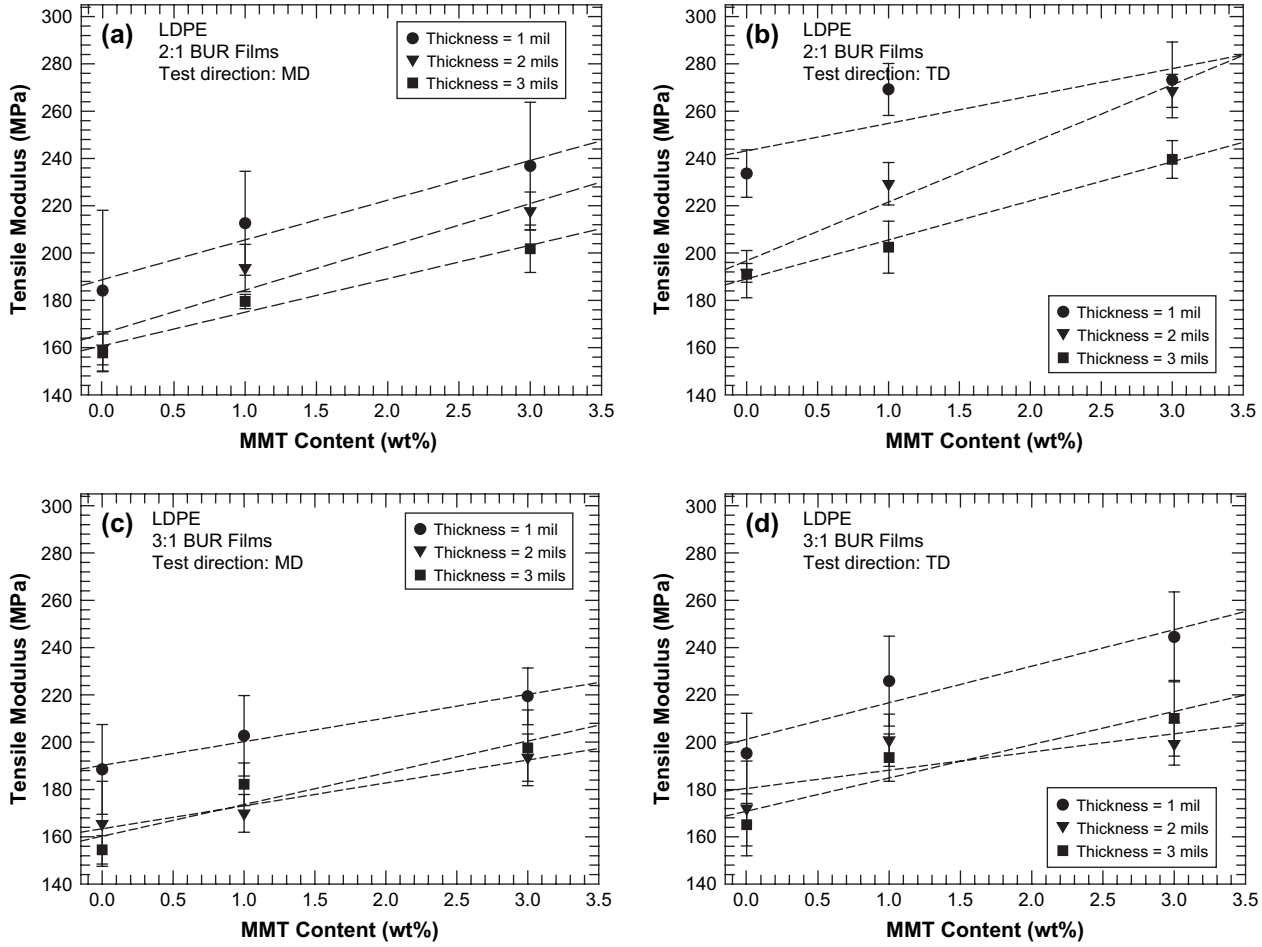

Fig. 3. Tensile modulus of blown films prepared from LDPE and $M_2(HT)_2$-140 organoclay plotted as a function of the montmorillonite content: (a) films with 2:1 BUR tested along the machine direction, (b) films with 2:1 BUR tested along the transverse direction, (c) films with 3:1 BUR tested along the machine direction, and (d) films with 3:1 BUR tested along the transverse direction. The abscissa has been extended beyond zero in all graphs for clarity. The dotted lines are trend lines (linear regression lines) and are included to serve as visual guides.

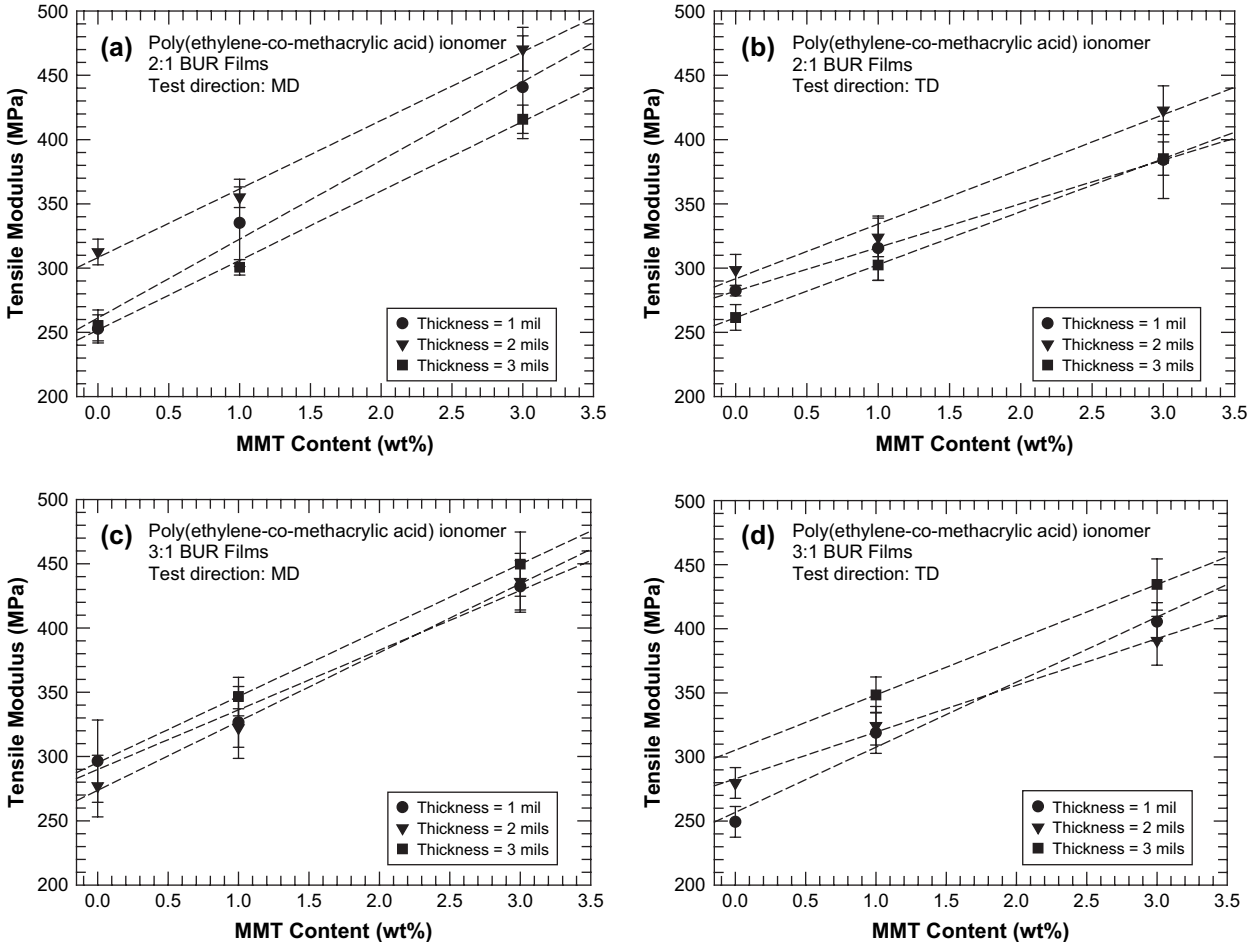

Fig. 4. Tensile modulus of blown films prepared from Surlyn® ionomer and $M_2(HT)_2$-140 organoclay plotted as a function of the montmorillonite content: (a) films with 2:1 BUR tested along the machine direction, (b) films with 2:1 BUR tested along the transverse direction, (c) films with 3:1 BUR tested along the machine direction, and (d) films with 3:1 BUR tested along the transverse direction. The abscissa has been extended beyond zero in all graphs for clarity. The dotted lines are trend lines (linear regression lines) and are included to serve as visual guides.

modulus of the films prepared from the ionomer based nanocomposites is significantly higher than that of the LDPE based nanocomposites. This is a result of better organoclay exfoliation in the ionomer than in LDPE as described earlier. A numerical comparison between the improvements in modulus exhibited by the nanocomposite films (containing 3 wt% MMT) prepared from LDPE and the ionomer relative to the corresponding films prepared from the unfilled polymer is presented in Table 3.

A comparison between Fig. 3(a) and (b) indicates that blown films prepared from unfilled LDPE have a higher tensile modulus along the transverse direction than along the machine direction. On the other hand, such trends are not evident in films prepared from the ionomer (Fig. 4). These results could be attributed to differences in crystallinity between the two polymers and orientation of the lamellae in these films. LDPE is considerably more crystalline than the ionomer (see Table 1); the bulky methacrylic acid groups of the ionomer interfere with the chain folding process, which subsequently results in a lower crystallinity and smaller crystallites compared to the base polyethylene. Thus, the ionomer has better optical properties, viz., haze, gloss, and clarity, than LDPE. Crystallization in a blown film process occurs under the influence of an external strain which generally results in an oriented morphology, with the long axes of the crystalline lamellae generally oriented perpendicular to the film MD. For polymers such as LDPE, the unit cell '*a*' axis is oriented preferentially along the film MD, and such a microstructure is

Table 3
Improvement in tensile modulus of blown films prepared from nanocomposites of LDPE and poly(ethylene-*co*-methacrylic acid) containing 3 wt% MMT relative to modulus of blown films produced using identical processing conditions from the corresponding unfilled polymers

Thickness (mil)	BUR	LDPE nanocomposite films		Ionomer nanocomposite films	
		% Improvements		% Improvements	
		MD	TD	MD	TD
1	2:1	29	17	74	36
2	2:1	36	40	51	42
3	2:1	28	25	63	47
1	3:1	17	23	46	63
2	3:1	17	17	57	40
3	3:1	28	27	NA	NA

well described by the Keller–Machin 'row' structure [25–27]. The orientation of the lamellar long axes perpendicular to the film MD causes the TD modulus to be higher than the MD modulus [28]. On the other hand, for nanocomposites prepared from the ionomer, tensile modulus is slightly higher in the MD than in the TD (opposite of nanocomposites based on LDPE). This is attributable to: (i) very low crystallinity in the ionomer films, and (ii) orientation of the clay platelets/tactoids in the plane of the film. The montmorillonite platelets are not perfectly circular, i.e., they have a major and a minor axis [29]. During the film blowing process, the major axis would tend to get aligned in the machine direction (more so at a lower BUR than at a higher BUR), and this would result in a higher modulus in the MD than the TD. In LDPE–organoclay composites, the level of organoclay exfoliation is not as great as that in the ionomer. As a result, the contribution of the orientation of the small aspect ratio filler particles towards the tensile modulus of the composite is more than negated by the contribution of the orientation of the crystal lamellae. On the other hand, in ionomer–organoclay nanocomposites, the polymer crystallinity is comparatively lower and the contribution of the orientation of the high aspect ratio clay particles dominates the tensile modulus values.

Another trend seen in Fig. 3 is that for LDPE based films, modulus increases as the film thickness decreases (increasing draw down ratio). This is true for the unfilled polymer and the nanocomposites. Films prepared from the ionomer or its nanocomposites do not reveal this trend (Fig. 4). Once again, this could be attributed to the differences in crystallinity between the two polymers and the consequent influence of the orientation of the crystal lamellae. For LDPE, greater orientation of the crystallites in the plane of the film, resulting from the elongational flow-induced morphology generated during the film blowing process, improves as the film thickness decreases.

3.3.2. Tensile stress at break

Tensile stress at break results for the blown films prepared from LDPE and its nanocomposites are presented in Fig. 5. Similar data for blown films prepared from the Surlyn® ionomer are presented in Fig. 6. In general, the ionomer films display greater tensile stress at break compared to the LDPE films. The presence of clay does not appear to change the

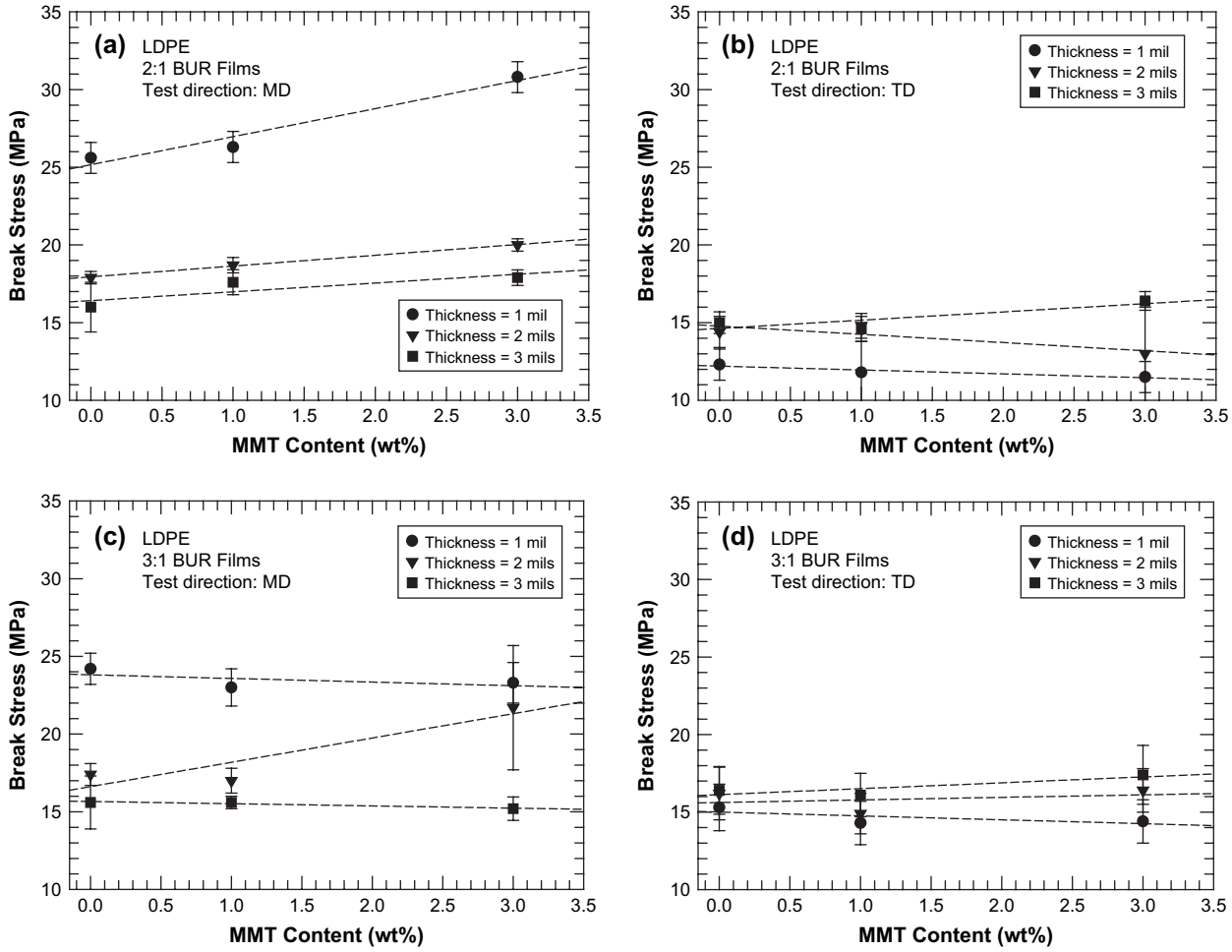

Fig. 5. Tensile stress at break of blown films prepared from LDPE and $M_2(HT)_2$-140 organoclay plotted as a function of the montmorillonite content: (a) films with 2:1 BUR tested along the machine direction, (b) films with 2:1 BUR tested along the transverse direction, (c) films with 3:1 BUR tested along the machine direction, and (d) films with 3:1 BUR tested along the transverse direction. The abscissa has been extended beyond zero in all graphs for clarity. The dotted lines are trend lines (linear regression lines) and are included to serve as visual guides.

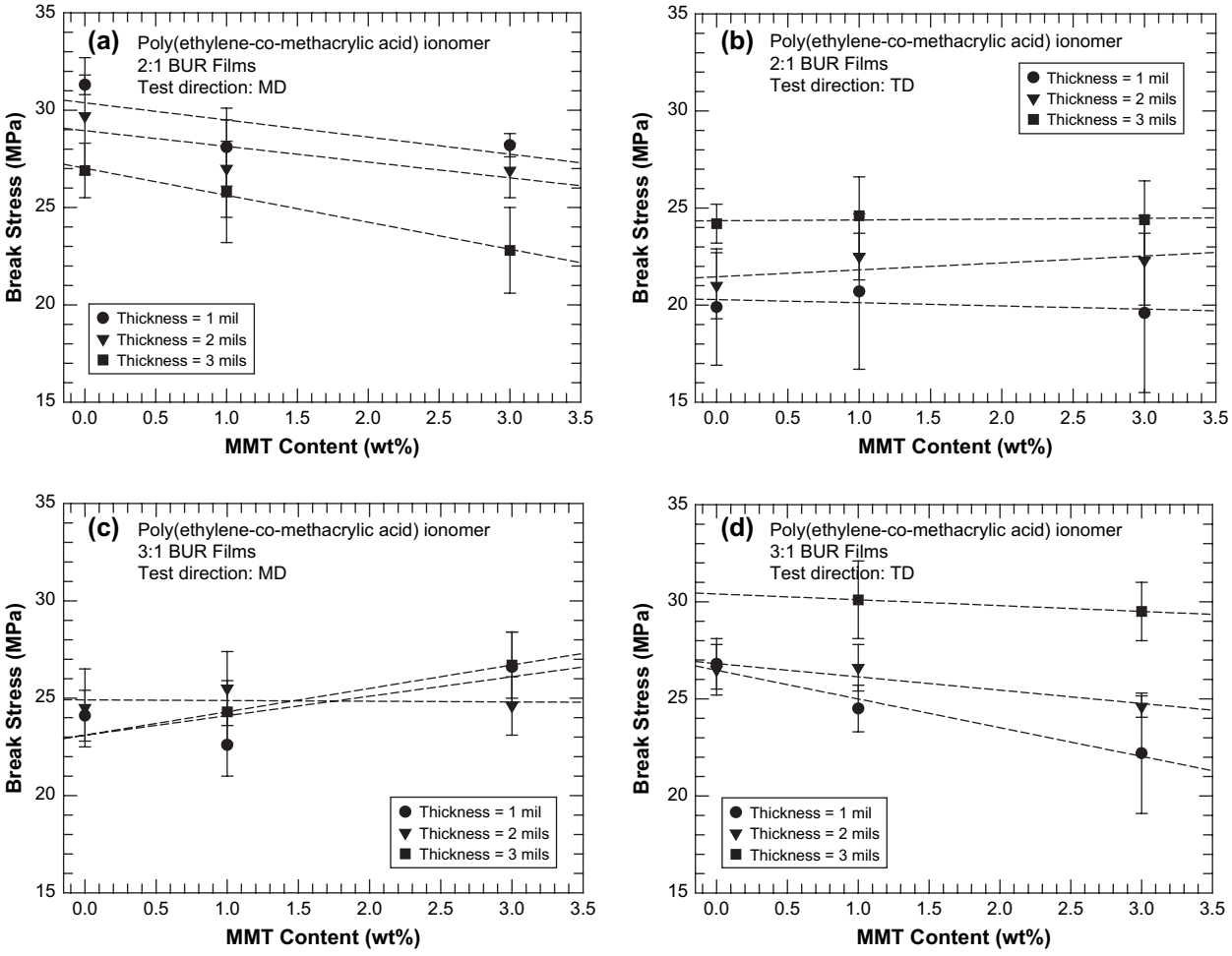

Fig. 6. Tensile stress at break of blown films prepared from Surlyn® ionomer and $M_2(HT)_2$-140 organoclay plotted as a function of the montmorillonite content: (a) films with 2:1 BUR tested along the machine direction, (b) films with 2:1 BUR tested along the transverse direction, (c) films with 3:1 BUR tested along the machine direction, and (d) films with 3:1 BUR tested along the transverse direction. The abscissa has been extended beyond zero in all graphs for clarity. The dotted lines are trend lines (linear regression lines) and are included to serve as visual guides.

tensile stress at break (along MD or TD) of the blown films prepared from either polymer.

In most cases, the stress at break in the machine direction is greater than that in the transverse direction. The effects are more pronounced at a lower blow-up ratio, and for the 1 mil thick films. Generally, in LDPE blown films with the 'row' structure, the MD stress at break tends to be higher than that along the TD [28]. Because this relates to the preferential orientation of the lamellar long axes perpendicular to the film MD, the differential in the break stress along the MD and TD is greater at lower BUR and for thinner films.

3.3.3. Tensile strain at break

Tensile strain at break results for blown films prepared from LDPE and its nanocomposites are presented in Fig. 7. Similar data for blown films prepared from the Surlyn® ionomer are presented in Fig. 8. It seems that the presence of clay does not affect the tensile strain at break (along MD or TD) of the blown films prepared from either polymer.

For LDPE and its nanocomposites, the strain at break in the transverse direction is higher than that in the machine direction. The ionomer and its nanocomposites also reveal a similar trend, but to a smaller extent. As expected, in all cases the strain at break increases with an increase in the film thickness.

3.3.4. Puncture resistance

Results of dart impact analysis (measure of puncture resistance) for blown films prepared from LDPE and its nanocomposites are presented in Fig. 9. Similar data for blown films prepared from the Surlyn® ionomer are shown in Fig. 10. In general, films prepared from the ionomer and its nanocomposites have higher impact strength than the corresponding films prepared from LDPE. The addition of clay lowers the dart impact strength of blown films of the two polymers.

For films prepared from LDPE and its nanocomposites, the dart impact strength for 3:1 BUR films is considerably greater than that of the 2:1 BUR films. Ionomer based films show similar trends, but to a lesser extent. These observations could be a result of higher biaxial orientation of the crystallites/clay platelets in the plane of the film when the BUR is increased from 2:1 to 3:1 [30].

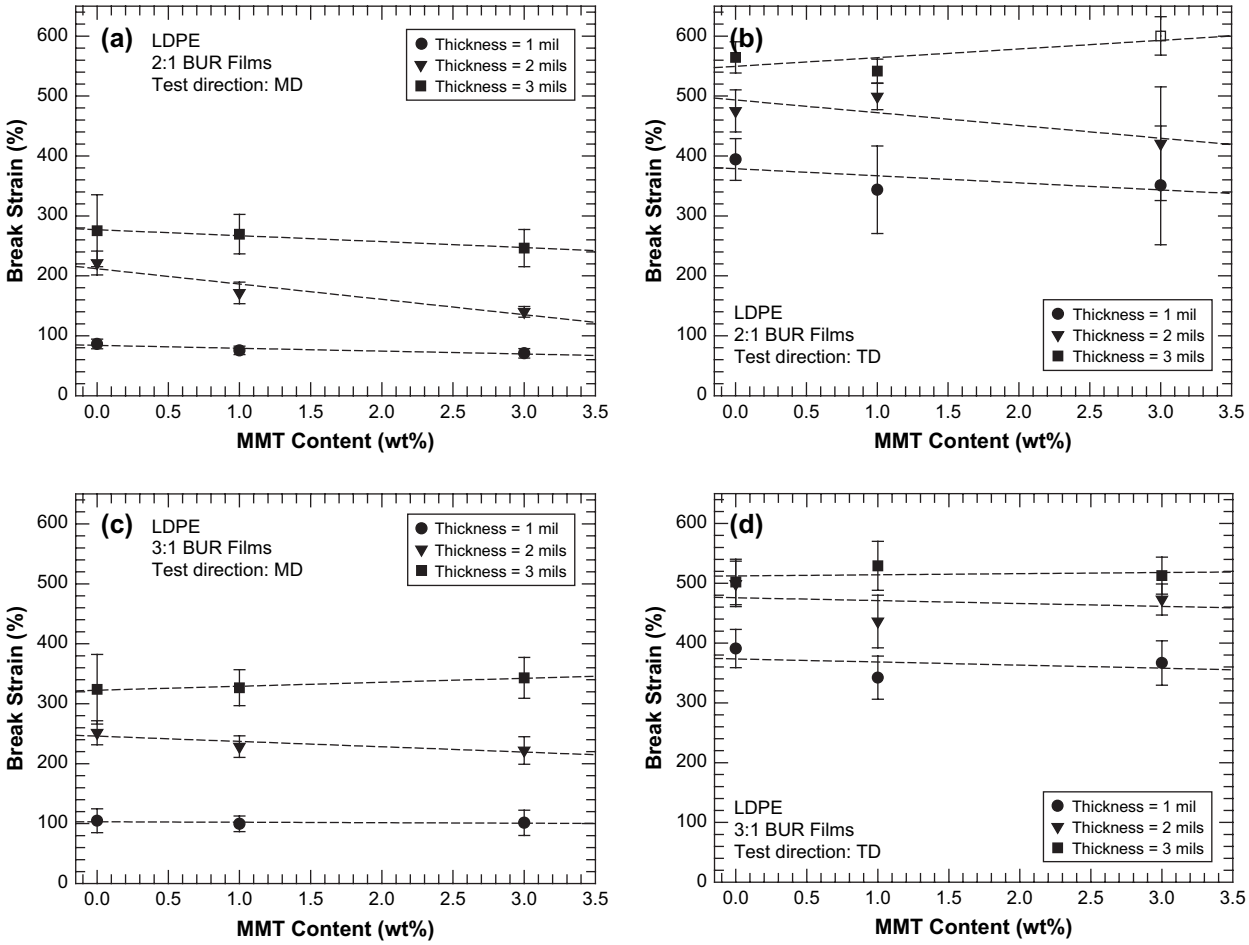

Fig. 7. Tensile strain at break of blown films prepared from LDPE and $M_2(HT)_2$-140 organoclay plotted as a function of the montmorillonite content: (a) films with 2:1 BUR tested along the machine direction, (b) films with 2:1 BUR tested along the transverse direction, (c) films with 3:1 BUR tested along the machine direction, and (d) films with 3:1 BUR tested along the transverse direction. The abscissa has been extended beyond zero in all graphs for clarity. The dotted lines are trend lines (linear regression lines) and are included to serve as visual guides.

3.3.5. Resistance to tear propagation

The tear resistance was measured along the machine direction and the transverse direction of the blown films. Results for films prepared from LDPE and its nanocomposites are presented in Fig. 11. Similar data for blown films prepared from the Surlyn® ionomer are presented in Fig. 12. One of the most noticeable observations is the difference between the tear strengths of the two polymers (and also their nanocomposites). The ionomer films display poor tear resistance relative to LDPE films. Although, it is not completely clear what could cause such a difference between the two systems, it could be a consequence of differences in crystallinity and orientation between the two polymers.

For unfilled LDPE films, the tear resistance is always higher along the MD relative to TD. This difference is more magnified at 2:1 BUR than at 3:1 BUR. This is very likely due to the varying degrees of orientation of the lamellae within the plane of the film. Both MD and TD tear resistance values are higher at 2:1 BUR relative to 3:1 BUR. A deeper insight into the lamellar morphology is required to explain this observation. However, such an investigation is beyond the scope of this study. Nanocomposites prepared from LDPE exhibited similar trends as the unfilled polymer. As the clay content increases, MD tear decreases and TD tear increases. This effect is more dramatic at higher DDR (1 mil thick films) than at lower DDR.

In contrast, tear resistance of films prepared from the ionomer and its nanocomposites seems fairly insensitive to the clay content. There is not much difference between the tear resistance in the machine direction and transverse direction for these films.

3.4. Barrier properties

3.4.1. Steady-state gas permeation properties

The measured gas permeability coefficients for selected blown films prepared from nanocomposites of LDPE and Surlyn® 8945 ionomer are tabulated in Table 4. The films were carefully chosen such that the effects of clay content and film blowing conditions on the permeability of these membranes to O_2, N_2, and CO_2 gases could be distinctly explored. A comparison between the gas permeabilities of the two unfilled polymer films (film #3 vs film #21, and film #6 vs film #24) shows that blown films prepared from the ionomer

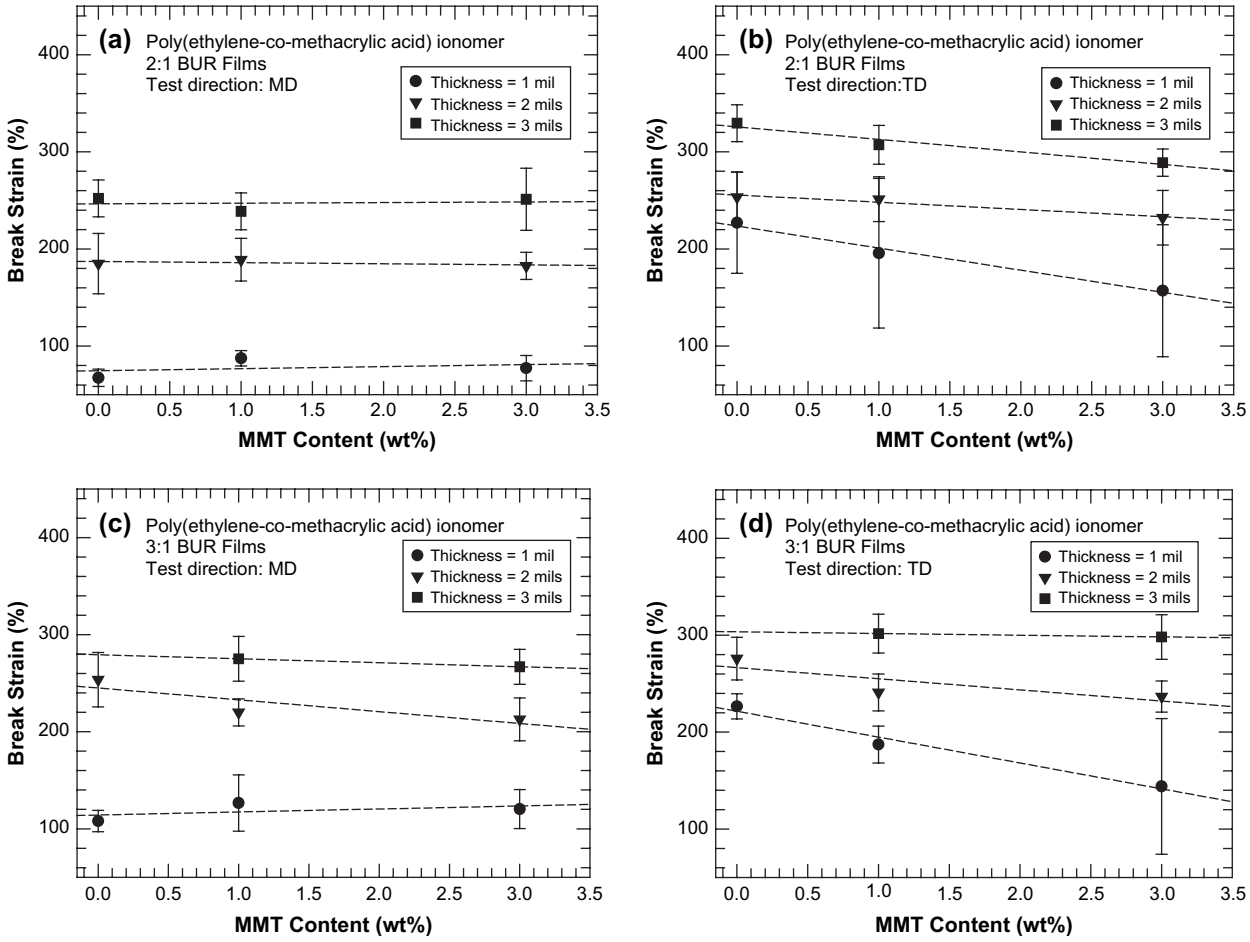

Fig. 8. Tensile strain at break of blown films prepared from Surlyn® ionomer and $M_2(HT)_2$-140 organoclay plotted as a function of the montmorillonite content: (a) films with 2:1 BUR tested along the machine direction, (b) films with 2:1 BUR tested along the transverse direction, (c) films with 3:1 BUR tested along the machine direction, and (d) films with 3:1 BUR tested along the transverse direction. The abscissa has been extended beyond zero in all graphs for clarity. The dotted lines are trend lines (linear regression lines) and are included to serve as visual guides.

have better barrier properties than those prepared from LDPE. In general, for polymers that are chemically identical, gas permeability increases as polymer crystallinity decreases [31]. However, in the case of the ionomer, the effects of the polar methacrylic acid groups and the sodium ion clusters more than compensate for the decreased barrier resistance brought by the lower crystallinity of the polymer relative to LDPE.

The permeability of the two polymers and their nanocomposites was much greater for CO_2 than O_2, which in turn was higher than the permeability of N_2. The differences between the permeability to various gases stem from the differences in diffusivity and solubility of the gas molecules in the polymer matrix. The permeability coefficient (P) is the product of the diffusion coefficient, D, and the solubility coefficient, S, i.e., $P = DS$. Diffusivity is governed by the size (e.g., critical volume) of a gas molecule. N_2 has a critical volume of 90 cm^3/mol compared to 74 cm^3/mol for O_2 and 94 cm^3/mol for CO_2. There is not a large difference between the solubilities of N_2 and O_2 [32]. Hence, the films have a higher permeability to oxygen than nitrogen. On the other hand, although the CO_2 molecule is larger than both oxygen and nitrogen, its solubility in the polymer membrane is significantly greater than that of the other two gases [32]. As a result, the polymer membranes have lower barrier resistance to CO_2 than O_2, and N_2.

Gas permeability decreases as the organoclay content increases in both polymers. The permeability coefficients of the nanocomposite films relative to the corresponding films without clay (P/P_0) for the various gases in LDPE and the ionomer nanocomposite films are also included in Table 4 (in parentheses). For a given polymer, at fixed montmorillonite content, there is not a significant difference between the relative permeabilities of the three gases. Hence, as an example, the relative permeability of CO_2 in LDPE and ionomer nanocomposite films is plotted as a function of the montmorillonite content in Fig. 13. At 1 wt% MMT, the relative permeabilities for the two polymer matrices are similar (within standard deviation). However, the nanocomposite film containing 3 wt% MMT prepared from Surlyn® 8945 ionomer shows a larger reduction in permeability compared to the corresponding film prepared from LDPE. This could be attributed to the superior level of organoclay exfoliation achieved in the ionomer compared to LDPE.

The effect of the draw down ratio on the barrier properties of blown films prepared from nanocomposites based on LDPE is shown in Fig. 14. It is clear that nanocomposite films with

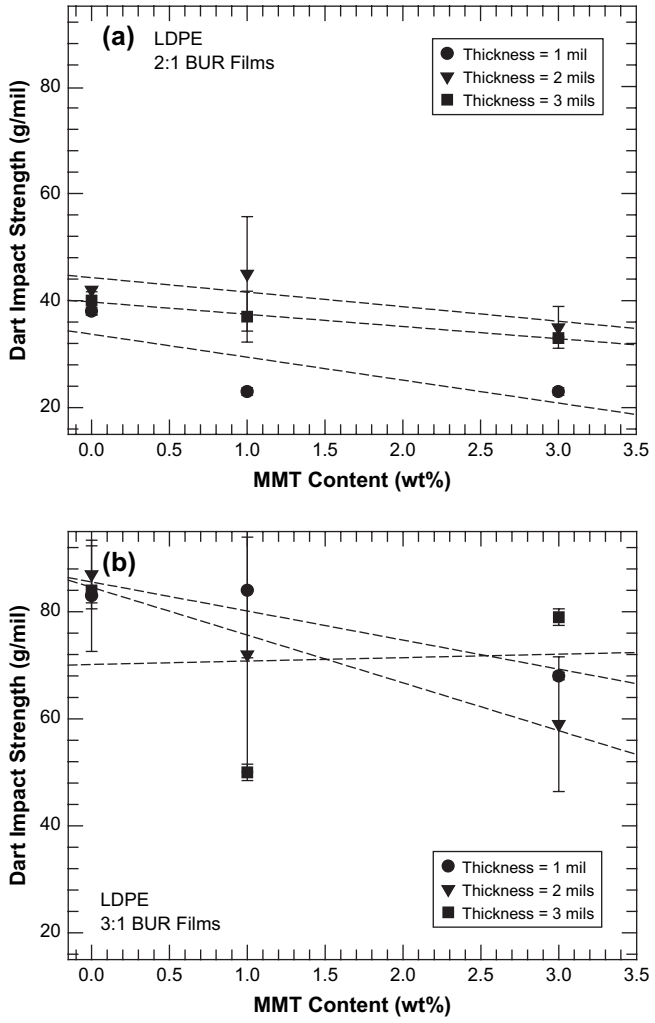

Fig. 9. Dart impact strength of blown films prepared from LDPE and $M_2(HT)_2$-140 organoclay plotted as a function of the montmorillonite content: (a) films with 2:1 BUR and (b) films with 3:1 BUR. The abscissa has been extended beyond zero in all graphs for clarity. The dotted lines are trend lines (linear regression lines) and are included to serve as visual guides.

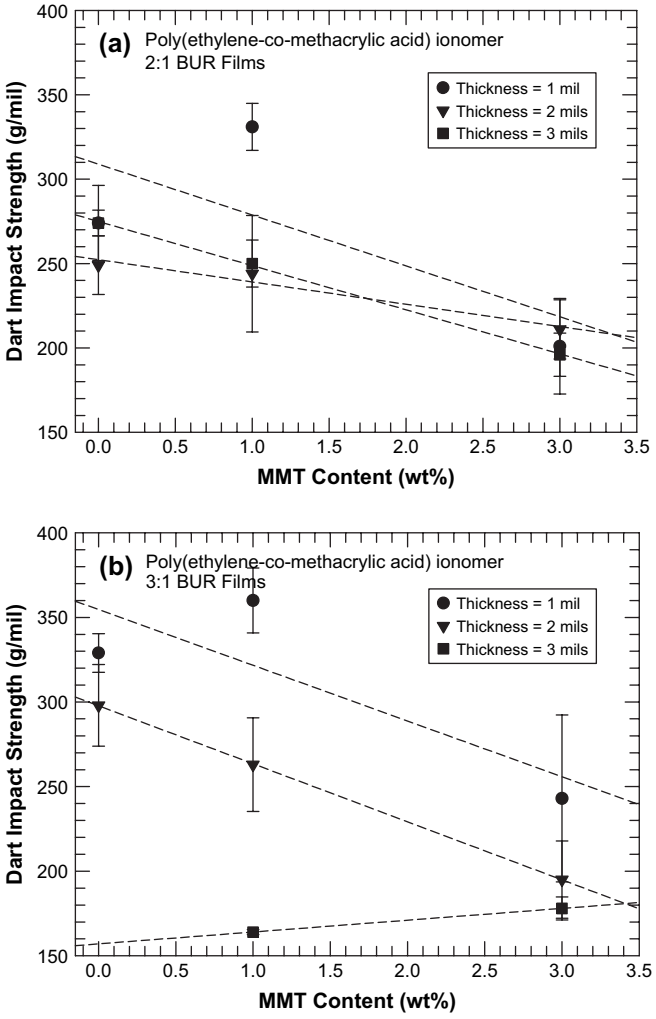

Fig. 10. Dart impact strength of blown films prepared from Surlyn® ionomer and $M_2(HT)_2$-140 organoclay plotted as a function of the montmorillonite content: (a) films with 2:1 BUR and (b) films with 3:1 BUR. The abscissa has been extended beyond zero in all graphs for clarity. The dotted lines are trend lines (linear regression lines) and are included to serve as visual guides.

greater DDR have superior gas barrier properties (per unit thickness) compared to those with smaller DDR. This could be due to possible greater biaxial orientation of the clay platelets in the plane of the film during the preparation of thinner films (large DDR) compared to thicker films (small DDR). Also, it seems that changing the BUR from 2:1 to 3:1 does not affect the relative gas permeabilities of the nanocomposite films prepared from either LDPE or the ionomer.

3.4.2. Comparison of steady-state permeation data with the Nielsen model

A number of theories have been proposed to correlate the gas permeability of composite membranes to the filler content and geometry [33–41]. In this study, we compare the experimental gas permeation data to that predicted by the tortuous path model proposed by Nielsen which approximates the filler particles as platelets with finite width, w, and thickness, t, but infinite length [33]. The mathematical form of this model is

$$\frac{P}{P_0} = \frac{(1-\phi)}{\left(1+\frac{\alpha\phi}{2}\right)}$$

where α = particle aspect ratio = w/t and ϕ = volume fraction of the particles.

Fig. 15 shows plots of the gas permeability coefficients for O_2, N_2, and CO_2 in the 1 mil thick nanocomposite films relative to the corresponding value for films prepared from the pure polymers. The solid lines represent the relative permeability, P/P_0, predicted for different particle aspect ratios by the Nielsen model. It is interesting to note that the aspect ratios of the particles in the ionomer and LDPE based nanocomposites determined using model calculations are significantly larger than those determined by the particle analysis technique ($\sim$10–30) [10,11,42]. Such a discrepancy could be a result of the assumptions built into the permeability model [33], and the problems associated with the calculation of the particle aspect ratio from TEM micrographs [42].

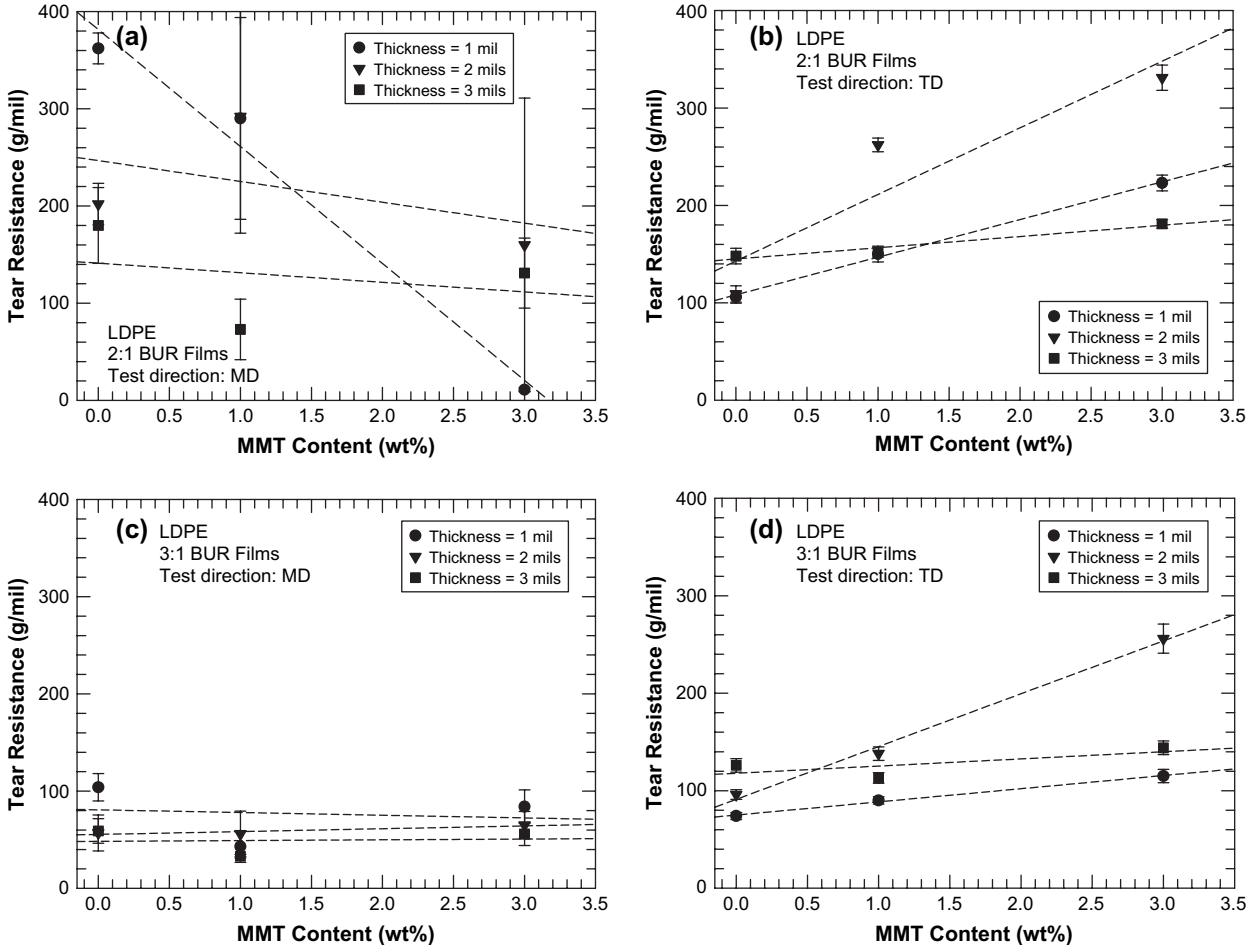

Fig. 11. Tear strength of blown films prepared from LDPE and $M_2(HT)_2$-140 organoclay plotted as a function of the montmorillonite content: (a) films with 2:1 BUR tested along the machine direction, (b) films with 2:1 BUR tested along the transverse direction, (c) films with 3:1 BUR tested along the machine direction, and (d) films with 3:1 BUR tested along the transverse direction. The abscissa has been extended beyond zero in all graphs for clarity. The dotted lines are trend lines (linear regression lines) and are included to serve as visual guides.

In a previous study, Hotta and Paul [9] determined the relative permeability of nanocomposite films containing 2.5 wt% MMT prepared from linear low density polyethylene (LLDPE) containing some maleated LLDPE as a compatibilizer to be ~0.8. These films were prepared by compression molding and were 150 μm thick; hence, it would not be fair to make a direct comparison between the films evaluated in the two studies. Nevertheless, a comparison of their data with the Nielsen model suggested a filler aspect ratio of ~60, which was also significantly larger than the aspect ratio of ~10 determined by particle analysis of the TEM micrographs. (Note: due to a calculation error, which came to the authors' attention after the publication of the manuscript, the theoretical relative permeability curves based upon the Nielsen model presented in that paper are incorrect.)

3.4.3. Moisture barrier properties

The water vapor transmission rate (WVTR) through the LDPE and ionomer films, measured as per ASTM F1249, is plotted as a function of the montmorillonite content in Fig. 16. The trends are similar to those observed for gas barrier properties, i.e., the reduction in WVTR with increasing montmorillonite content is greater for the ionomer film compared to the LDPE film. Once again, this could be attributed to the differences in the level of organoclay exfoliation of the two systems. It is noteworthy that although the level of organoclay exfoliation is relatively poor in LDPE [10,11], the addition of 3 wt% MMT lowers the WVTR by as much as 45%. The improvement in moisture barrier properties of similar nanocomposite films prepared from the ionomer is ~60%. The relative permeability values of the nanocomposite films for water vapor are somewhat different than those for the gases evaluated in the earlier section. Based upon the tortuous path model, there should not be any differences in the relative permeability for the gases and water vapor (assuming that the method used for testing does not have a significant bearing on the results). This is an interesting observation and should be a part of another broader investigation.

4. Conclusions

Mechanical and barrier properties of blown films prepared from nanocomposites based on LDPE and a sodium ionomer

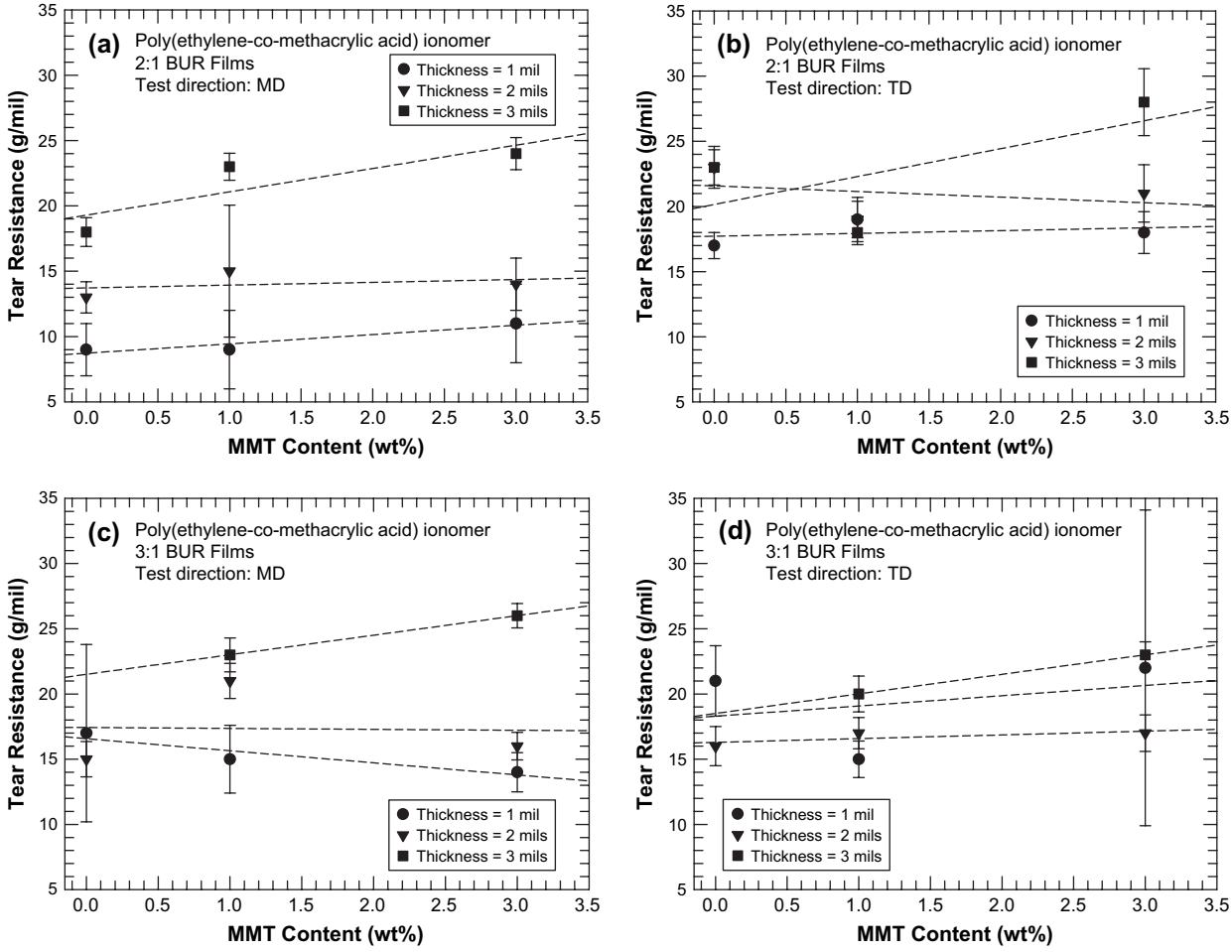

Fig. 12. Tear strength of blown films prepared from Surlyn® ionomer and $M_2(HT)_2$-140 organoclay plotted as a function of the montmorillonite content: (a) films with 2:1 BUR tested along the machine direction, (b) films with 2:1 BUR tested along the transverse direction, (c) films with 3:1 BUR tested along the machine direction, and (d) films with 3:1 BUR tested along the transverse direction. The abscissa has been extended beyond zero in all graphs for clarity. The dotted lines are trend lines (linear regression lines) and are included to serve as visual guides.

of poly(ethylene-*co*-methacrylic acid) are presented here. The organoclay and processing conditions were carefully chosen to form nanocomposites with acceptable levels of exfoliation. Films prepared from the nanocomposites had a smooth texture and surface properties; however, the haze increased slightly with increasing MMT content. In general, films prepared from nanocomposites based on the ionomer exhibited greater improvements in mechanical and barrier properties over unfilled polymer compared to similar films prepared from nanocomposites based on LDPE. This is due to the higher levels of

Table 4
Gas permeability data of selected blown films evaluated in this study[a]

Film no.	LDPE films			Permeability (barrer)[b]			Film no.	Ionomer films			Permeability (barrer)[b]		
	MMT	BUR	Thickness (mil)	O_2	N_2	CO_2		MMT	BUR	Thickness (mil)	O_2	N_2	CO_2
3	0	2:1	1	9.302	3.112	38.918	21	0	2:1	1	2.967	0.846	11.350
4	0	3:1	3	6.705	2.241	27.515							
5	0	3:1	2	6.348	2.171	27.357							
6	0	3:1	1	9.553	3.110	38.982	24	0	3:1	1	2.954	0.814	10.750
12	1	3:1	1	7.525 (0.788)	2.528 (0.813)	31.684 (0.813)	30	1	3:1	1	2.458 (0.832)	0.694 (0.852)	9.097 (0.846)
15	3	2:1	1	6.636 (0.713)	2.223 (0.714)	28.090 (0.722)	33	3	2:1	1	1.881 (0.634)	0.554 (0.655)	6.950 (0.612)
16	3	3:1	3	5.654 (0.843)	1.985 (0.886)	23.758 (0.863)							
17	3	3:1	2	5.318 (0.838)	1.788 (0.824)	22.485 (0.822)							
18	3	3:1	1	6.597 (0.691)	2.278 (0.732)	28.270 (0.725)	36	3	3:1	1	1.765 (0.597)	0.502 (0.616)	6.645 (0.618)

[a] The values in parentheses are the permeabilities of the three gases in nanocomposite films relative to those in the corresponding unfilled polymer films (P/P_0). Comparable films made from the ionomer and LDPE are listed side by side.

[b] 1 Barrer $= 10^{-10}$ cm^3 (STP) cm/(s cm^2 cmHg).

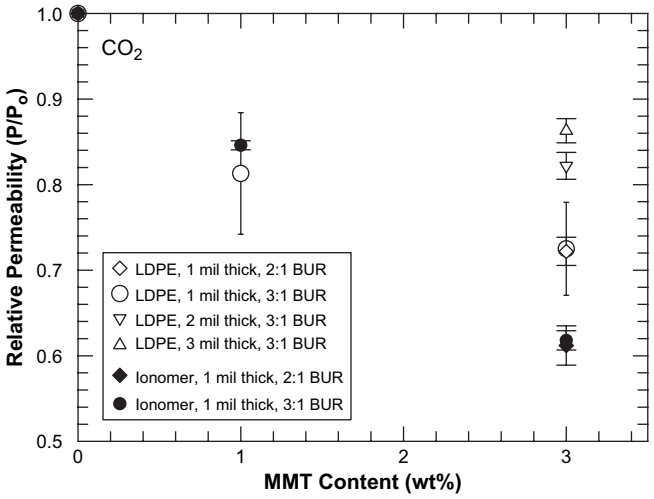

Fig. 13. Relative permeability (P/P_0) of CO_2 gas plotted as a function of the montmorillonite content of the nanocomposite films prepared from LDPE (open symbols) and Surlyn® 8945 ionomer (filled symbols).

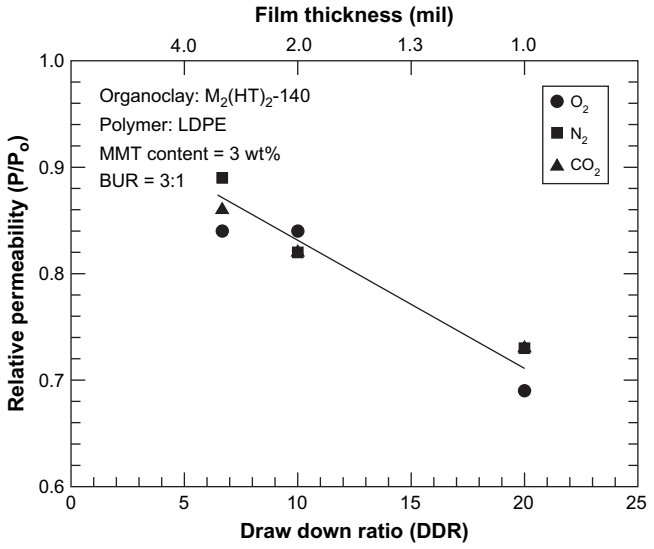

Fig. 14. Effect of draw down ratio (DDR) on the barrier properties of blown films prepared from nanocomposites based on LDPE.

organoclay exfoliation achieved in the ionomer compared to LDPE.

The tensile modulus of blown films based on the ionomer increased by an average of 50% without sacrificing tear strength, puncture resistance or film extensibility upon addition of 3 wt% MMT to the polymer. In contrast, the same amount of organoclay resulted in a 25% increase (average) in the modulus of LDPE films. Mechanical properties of films prepared from LDPE and its nanocomposites were more sensitive to processing conditions than those prepared from the ionomer and its nanocomposites. This is because LDPE is more crystalline than the ionomer, and the orientation of the crystal lamellae also plays a role (besides that played by the clay platelets) in the determination of the mechanical properties.

The nanocomposites also offered significant improvements in barrier properties compared to the corresponding unfilled

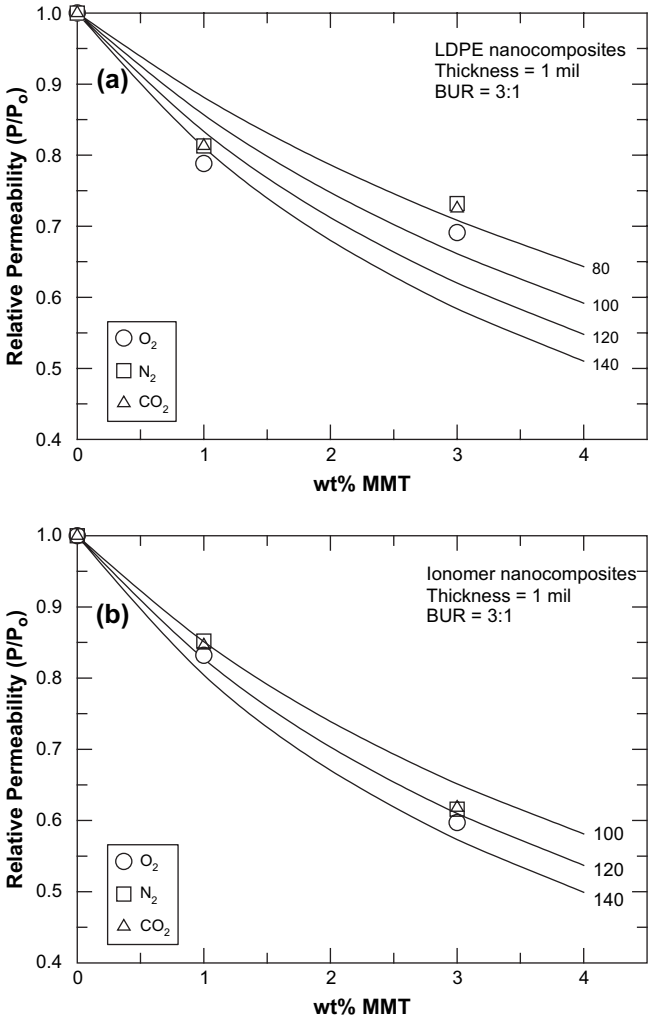

Fig. 15. Relative permeability of O_2, N_2, and CO_2 in nanocomposite films prepared from (a) LDPE and (b) Surlyn® 8945 ionomer. The solid lines represent predictions via the Nielsen equation for different values of particle aspect ratio; this model assumes all platelets are perfectly aligned in the plane of the film.

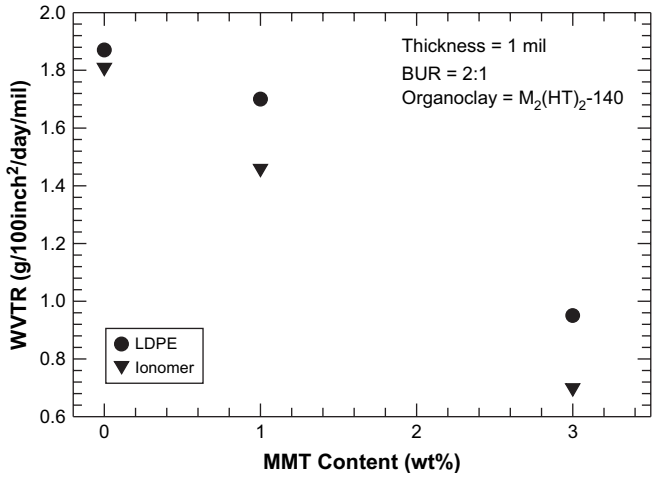

Fig. 16. Water-vapor transmission rate (WVTR) of blown films prepared from LDPE and Surlyn® ionomer plotted as a function of the montmorillonite content: the abscissa has been extended beyond zero for clarity.

polymers. Gas permeability of ionomer films was lowered by as much as 40% and moisture transmission rate was lowered by 60% upon addition of 3 wt% MMT to the polymer. The improvements in barrier properties of LDPE based nanocomposite films were relatively smaller owing to lower levels of exfoliation.

Acknowledgements

We sincerely thank Doug Hunter and Southern Clay Products Inc. for providing organoclay materials and several insightful discussions. We also acknowledge Ben Knesek, David Higbee, and Jerry Stark for their help during melt processing of nanocomposites.

References

[1] Avella M, De Vlieger JJ, Errico ME, Fischer S, Vacca P, Volpe MG. Food Chemistry 2005;93(3):467–74.
[2] Gain O, Espuche E, Pollet E, Alexandre M, Dubois P. Journal of Polymer Science, Part B: Polymer Physics 2004;43(2):205–14.
[3] Incarnato L, Scarfato P, Russo GM, Di Maio L, Iannelli P, Acierno D. Polymer 2003;44(16):4625–34.
[4] Jacquelot E, Espuche E, Gerard JF, Duchet J, Mazabraud P. Journal of Polymer Science, Part B: Polymer Physics 2005;44(2):431–40.
[5] Krook M, Albertsson AC, Gedde UW, Hedenqvist MS. Polymer Engineering and Science 2002;42(6):1238–46.
[6] Osman MA, Mittal V, Lusti HR. Macromolecular Rapid Communications 2004;25(12):1145–9.
[7] Barbee RB, Matayabas Jr JC, Trexler Jr JW, Piner RL, Gilmer JW, Connell GW, et al. US Patent 99-338222, 6486252; 2002 [Assigned to (Eastman Chemical Company, USA)].
[8] Presenz U, Sutter AM. Application: WO Patent 2003-CH77, 2003064503; 2003 [Assigned to (EMS-Chemie A.-G., Switz.)].
[9] Hotta S, Paul DR. Polymer 2004;45(22):7639–54.
[10] Shah RK. Ph.D. dissertation, The University of Texas at Austin; 2006.
[11] Shah RK, Paul DR, in preparation.
[12] Eisenberg A, Kim J-S. Introduction to ionomers. New York: Wiley; 1998. 327 p.
[13] Shah RK, Hunter DL, Paul DR. Polymer 2005;46(8):2646–62.
[14] Lee JA, Kontopoulou M, Parent JS. Polymer 2005;46(14):5040–9.
[15] Manufacturer's information, at http://www2dupontcom/Surlyn/en_US/uses_apps/, E.I. du Pont de Nemours and Company.
[16] Wunderlich B. Macromolecular physics. In: Crystal melting, vol. 3. New York: Academic Press; 1980. p. 47–58.
[17] Hunter DL. Personal communication.
[18] Chavarria F, Paul DR, in preparation.
[19] Koros WJ, Paul DR, Rocha AA. Journal of Polymer Science, Part B: Polymer Physics 1976;14(4):687–702.
[20] Krishnamoorti R, Silva AS. Polymer–clay nanocomposites. In: Pinnavaia TJ, Beall GW, editors. John Wiley & Sons; 2000. p. 315–43.
[21] Krishnamoorti R, Ren J, Silva AS. Journal of Chemical Physics 2001;114(11):4968–73.
[22] Zhong Y, De Kee D. Polymer Engineering and Science 2005;45(4):469–77.
[23] Xu L, Reeder S, Thopasridharan M, Ren J, Shipp DA, Krishnamoorti R. Nanotechnology 2005;16(7):514–21.
[24] Chevron Phillips Chemical Company. Personal communication.
[25] Krishnaswamy RK. Journal of Polymer Science, Part B: Polymer Physics 2000;38(1):182–93.
[26] Pazur RJ, Purd'homme RE. Macromolecules 1996;29(1):119–28.
[27] Keller A, Kolnaar HWH. Processing of polymers. In: Cahn RW, Haasen P, Kramer EJ, editors. Materials science and technology, vol. 18. John Wiley & Sons; 1997. p. 189–268.
[28] Krishnaswamy RK, Lamborn MJ. Polymer Engineering and Science 2000;40(11):2385–96.
[29] Lee KY, Paul DR. Polymer 2005;46(21):9064–80.
[30] Krishnaswamy RK, Sukhadia AM. Journal of Plastic Film and Sheeting 2005;21(2):145–58.
[31] Michaels AS, Bixler HJ. Journal of Polymer Science 1961;50:393–412 and 413–39.
[32] Ghosal K, Freeman BD. Polymers for Advanced Technologies 1994;5(11):673–97.
[33] Nielsen LE. Journal of Macromolecular Science, Part A 1967;1(5):929–42.
[34] Lape NK, Nuxoll EE, Cussler EL. Journal of Membrane Science 2004;236(1–2):29–37.
[35] Perry D, Ward WJ, Cussler EL. Journal of Membrane Science 1989;44(2–3):305–11.
[36] Lape NK, Yang C, Cussler EL. Journal of Membrane Science 2002;209(1):271–82.
[37] Bharadwaj RK. Macromolecules 2001;34(26):9189–92.
[38] Falla WR, Mulski M, Cussler EL. Journal of Membrane Science 1996;119(1):129–38.
[39] Yang C, Smyrl WH, Cussler EL. Journal of Membrane Science 2004;231(1–2):1–12.
[40] Gusev AA, Lusti HR. Advanced Materials (Weinheim, Germany) 2001;13(21):1641–3.
[41] Fredrickson GH, Bicerano J. Journal of Chemical Physics 1999;110(4):2181–8.
[42] Shah RK, Paul DR. Macromolecules 2006;39(9):3327–36.